Original Article

Role Of Cardiac MRI In Evaluation Of Pediatric Surgically Corrected Congenital Heart Disease

Shaimaa Mahmoud El Sharaby [1]*, Sara Kamal El Fawal [2], Noha Mohamed Abd El Maboud [1], Mohamed Hassan El Shafey[1]

1. Radiodiagnosis Department, Faculty of Medicine, Tanta University, Tanta, Egypt.
2. Radiodiagnosis Department, Faculty of Medicine, Alexandria University, Alexandria, Egypt.

Email: shaimaaelsharaby@outlook.com
DOI: 10.47750/pnr.2023.14.S01.200

Abstract

Background: Imaging is fundamental to the diagnosis of congenital heart disease and is required at all stages of case care. Cardiac magnetic resonance imaging (CMRI) provides high-resolution, isotropic, three-dimensional data. The aim of this work was to assess role of CMRI in post-surgery evaluation of pediatric surgically corrected CHD.
Methods: This prospective research was carried out on 33 cases from 5 to 21 years old, referred postoperatively to be examined by CMRI examination. All cases were subjected to Echo and CMRI examination.
Results: The most frequent CHD coming for post-surgery evaluation was TOF which represented 42% of the cases. The common post-surgery complication in all interventions of TOF repair was PR found in 71% of cases after TAP while 14% on top of homograft PA conduit. Combined PA stenosis and PR found in 29% on top of TAP while 7% on top of homograft PA conduit. RV dysfunction found in (28.5%) on top of RV dilatation. The cases of single ventricle repair (27% of cases) with the common complication functional ventricular dysfunction in 44%. After TGA repair (15%), the common complications were PA branch stenosis (20%), PA valve stenosis (20%), LV dysfunction (40%). **Conclusions:** CMRI provides a powerful non-invasive imaging tool, giving anatomic and haemodynamic information that echo and catheterization alone don't provide, during post-surgical follow up of CHD.

Keywords: Cardiac MRI; Pediatric; Surgically Corrected; Congenital Heart Disease

INTRODUCTION

Congenital heart disease (CHD) has a birth prevalence of 6 to 8 per 1000[1]. Advances in early diagnosis (including fetal Echo) and treatment have led to an increase in the number of CHD cases who reach adulthood [2].
Over the past several decades, major advancements in paediatric cardiology and cardiac surgery have led to a marked improvement in survival rates for the majority of CHD types. During this time period, advances in surgical and medical remedies have emerged [3, 4].

The diagnosis of CHD can often be difficult [5]. Imaging is crucial to the diagnosis of CHD and is necessary at all stages of case care. From the stage of fetal development onwards, imaging that clarifies anatomy and physiology, aids in refining management, evaluates the outcomes of interventions, and aids in prognosis [2].
A perfect technique used for visualization of CHD should be able to identify all features of the anatomy, including abnormalities of heart and great vessels, assess physiological impacts of CHD such as measurement of the blood flow across valves or blood vessels, be economical and portable, not cause overbearing distress and morbidity, and not expose cases to harmful ionizing radiation [6].

However, no single imaging modality meets these requirements for all cases and diseases [2]. Consequently, the evaluation of CHD must incorporate a number of techniques that can be utilized in a complementary manner. CMRI provides anatomical and physiological information that Echo and catheterization alone are incapable of providing [8].
Our research was the first cardiac MR research performed in our institution to assess the CHD post-surgery. The aim of this work was to assess the role of cardiac magnetic resonance imaging (CMRI) in post-surgery evaluation of pediatric surgically corrected CHD.

Patients and Methods

This prospective research was carried out on 33 cases aged from 5 to 21 years old, referred postoperatively from the cardiothoracic surgery and cardiology departments to be examined by CMRI examination for a clinically necessary standard of care after surgical repair between June 2017 and June 2021. The research was done after approval from the

institutional Ethical Committee. Informed consent for use of the data was obtained from all subjects or respectively their parents prior the CMRI examination.
Exclusion criteria were hemodynamic instability or acute respiratory insufficiency and any contraindication to MRI in general as pacemakers (particularly older types), any type of ear implant, metallic ocular foreign body and implanted insulin pump.
All cases were subjected to complete history taking (present, past and surgical history), clinical examination (general and local examination), ECG monitoring, Echo and renal function test and cardiac MRI examination.

Technique of CMRI imaging
Before the examination, the interventions of the examination were explained to the children's parents or to the older cases themselves including breath-hold instructions. All undergarments containing metal were removed. Infants and young children up to the age of 4 were anesthetized, whereas older children were examined with no anaesthesia. The sedation techniques included medication by oral chloral hydrate (75 mg/kg body weight) or midazolam, ketamine injection or propofol infusion.

Magnetic resonance scanner
This study utilized a 1.5 Tesla whole-body MR imaging device. (Philips Healthcare). Each patient was checked while lying flat. An ECG was recorded by attaching four electrodes to the patient's chest wall anteriorly. After making sure the QRS complex could be seen on the ECG, the placement of the leads was fine-tuned. On the MRI machine, the patient's pulse rate was also tracked. Scanning were executed using non-breath holding methods, while with older children cases undergoing breath-holding scan techniques based on accurate monitoring of diaphragmatic movement using breathing sensor which was positioned over the abdomen or thorax. For this purpose, we employed a phased-array body surface coil with six elements.

Cardiac MRI protocol and standard parameters:
Scout images in the three orthogonal planes (axial, sagittal and coronal) were gained during free breathing and not gated to the ECG for planning of the long and short axis view.

ECG gated, balanced steady-state free-precession (SSFP), white blood cine images were acquired in standard trans-axial (chest) view, two-chamber, four-chamber, short-axis views, LVOT as well as RVOT. For ventriculography cine images that enabled calculation of ventricular volume, mass, and ejection fraction as well as evaluation of regional wall motion. When possible, breath-hold acquisitions were done. Alternatively, free breathing imaging with multiple signal averaging (2–4) was performed or respiratory-navigator gating. Acquisition parameters were: TE= 2.3 ms, TR= 4.7 ms, FOV 300 mm, Matrix 240 x 256 mm, slice thickness with infants 2.74 mm and with older Children 6-8 mm, interslice gap= 1.37 mm, Phases: 25, flip angle 90°.

Free respiratory navigator and ECG -gated 3D steady state free precession sequence (SSFP), 3D anatomic dataset without the utilization of a contrast agent. Using ECG triggering, data acquisition was limited to one or two segments of the cardiac cycle in order to reduce distortion caused by cardiac mobility. The 3D SSFP sequence was executed with unrestricted respiration. By gating data acquisition with expiration while using a navigator beam to monitor the motion of the diaphragm, respiratory movement was compensated. (Navigator window was 3 mm.). Acquisition parameters were: TE= 2.3 ms, TR= 4.7 ms, FOV 300 mm, Matrix 240 x 256 mm, slice thickness= 2.74 mm, interslice gap= 1.37 mm, flip angle 90°. To acquire systolic and diastolic datasets, we identified the right trigger delay in a 4-chamber-cine-sequence (SSFP single slice) by manual tracing of the end-systole and end-diastole. The trigger Delay was in Diastole.

The contrast enhanced MR-angiography (ceMRA) of the aorta / PA biphasic including MIP reconstructions, CeMRA was acquired using a dose of 0.1-0.2 mmol/kg of contrast medium Gadobutrol, administered intravenously with a flow of 3 ml/sec, followed by a standard bolus of 50 ml NaCl with a flow of 3 ml/sec. The acquisition was started manually “on sight” as the contrast medium accumulated in the RV. Data sets were acquired without ECG-gating. Imaging parameters were: TE= 1.14 ms, TR= 2.5 ms, FOV 480 mm, ACQ-Matrix 424 x 372 mm, slice thickness= 3 mm, interslice gap= 1.5 mm, flip angle 30°.

Flow images were performed via Velocity-encoded phase-contrast (PC) cine CMRI (VENC),Was done to quantify the flow measurement over the MPA and AAO and the LPA/RPA each tp, the MPA ip/tp. Velocity encoding sensitivity (VENC) was adapted to the expected velocities (Starting from 200 cm/sec for aortic flow and 150 cm/sec for PA flow and increased by 50 cm/sec until there is no aliasing). FOV 320 mm, slice thickness of 7mm, interslice gap= 7 mm, TR/TE 5.1/3.04 msec and flip angle 15-30°, matrix 256 x 128. Navigator-based non-breath hold techniques were applied to improve the temporal or spatial resolution.

The late gadolinium enhancement sequence (LGE) is performed ten to twenty minutes after the administration of 0.1–0.2 mmol/kg of a GBCA that was used to perform an MRA. Contiguous short-axis imaging planes (from base to

apex) and a long-axis imaging plane were used to acquire images with LGE. To facilitate comparison, imaging planes and slice thickness matched those used for cine imaging of the ventricles.
According to the disease, additional case-specific and comprehensive imaging was acquired.

Functional single ventricle after Fontan operation in addition to standard imaging, Cine (SSFP) CMRI: coronal or oblique stack to image Fontan obstruction in long-axis and PC. (Phase Contrast) CMRI: Aao (neu Ao rather than nativ Ao after Norwood Op), branch PAs, Fontan Conduit (ip/tp), SVC, IVC

TOF following total correction: Adding to the Standard imaging, Cine CMRI: stack of images parallel to the long axis of the RVOT and PA valve
D-loop transposition of the great arteries after repair in addition to routine imaging, the following were collected: Cine SSFP: axial stack from the midliver to the aortic arch, CE-MRA or 3D SSFP for imaging the thoracic vasculature, and systemic and PA venous obstructions.

Image analysis and interpretation:
All acquired images were transferred to a post-processing workstation and image analysis. Measurements were performed with Philips software by two radiologists, each with >2 years of experience in post-processing.

Statistical analysis
Data were collected and entered to Excel Sheet then analyses were performed using SPSS version 21. Quantitative data were presented by Mean ± SD, range, median and Interquartile range (IQR). Categorical data were presented by number and percent.

Results

The present research included 33 cases their age ranged from 5-21 years old with a mean (±SD) of 13.5 ± 2.12years, 18 (54.5%) of cases were male and 15 (45.5%) of cases were female.
The 42.42 % of the cases (n=14) underwent post TOF repair, 15.15% (n=5) underwent post d-transposition of the great vessels (TGA) repair, 27.27% of the cases (n=9) underwent single ventricle repair, and finally 15.15% (n=5) underwent other different operations; 9% (n=3 cases) with congenital aortic valve stenosis underwent Ross operation and 3% for each of PA and VSD with LtmBT shunt and ASD closure.

Regarding the different subtypes of CHD with associated surgical interventions in our research, in post TGA repair cases; 3 diagnosed with d-TGA and 2 diagnosed with Double outlet right ventricle (DORV) TGA type. Four of them underwent Arterial switch LeCompte-maneuver while one of them underwent atrial switch (Senning intervention). While in single ventricle cases; 5 cases (55.6%) of them diagnosed with HLHS and one case with DILV underwent three stage surgical operation of Norwood operation, 2 cases (22.2%) diagnosed with HRHS and one case diagnosed with DORV underwent surgical repair through Glenn and Fontan. All TCPC was of extracardiac type. In the other hand 13 cases diagnosed with TOF while one with DORV Fallot type. 12 cases repaired with the traditional TAP (transannular Patch) and 2 of cases repaired with Conduit insertion in the PA position; one of Homograft Type and the other with Stented Xenograft type **(Table 1).**

There were different complications detected in the different post-surgery interventions performed in various CHD, in cases post TGA repair, RV dilation and failure found in the case who had Senning intervention. However after ASO the followings were detected PA branch stenosis (in 20%), reisthmus stenosis with PA valve stenosis (in 20%), and LV dysfunction (in 40%). In other hand after Single ventricle repair (9 cases), functional ventricular dysfunction in 44% (n=4) and 22% (n=2) showed lesions in previous site of operation as LSA occlusion from previous mBT and re isthmus stenosis. Near total cases of single ventricle repair (77%) developed dilation of new/ nativ aorta. Patent TCPC with no stenosis or thrombosis found in 100% of cases **(Table 2).**

Regarding complications detected after TOF repair, PR found in 71% of cases after TAP while 14% on top of homograft PA conduit. 50% of cases showed aneurysmal dilation of patch with significant PR (more than 40%). Combined PA stenosis and PR found in 29% (n=4) on top of TAP while 7% (n=1) on top of homograft PA conduit. PA branch stenosis was detected in 21% (n=3). 9 cases (64%) showed right ventricular dilation with six cases (42%) had marked dilatation; five of them (36%) with significant tricuspid regurgitation. RV dysfunction found in four cases (28.5%) on top of RV dilatation.

In case treated for PA atresia, showed biventricular significant dilation with slightly LV dysfunction **(Table 2).**
After Ross Operation 100% of cases showed aortic ectasia of average 45 mm. The other complication developed on top of the homograft PA conduit in 66.7% of the cases in the form of moderate PI with combined PA stenosis associated with moderate right ventricular dilatation with moderate TI. However RV dysfunction found only in one case (33.3%). No complications were detected in case after ASD closure **(Table 2).**

As regard the valve lesions seen in our research, after surgical repair d-TGA, three cases (60% of cases) had PR (RF less than 20%), while 20% (n=1) had combined PS. TI found in 60% of cases but only one case (20%) developed moderate TI 30%RF, this after Senning intervention. After single ventricle repair 55.6% of cases (n=5) had trivial degree AR less than 20% combined with new/ nativ aortic dilatation, three cases (33.3%) cases had TI, 11% mild degree and 11% of moderate degree. In post TOF repair 12 of cases (85.7%) had PR; 7 of them (50 %) severe grade (> 40 %), 4 cases moderate grade. Combined PS and PR found in five cases (35.8%). 10 cases (71.4%) showed TI with three of them (21.5%) severe grade and two (14 %) with moderate grade. Finally after Ross operation 2 of cases (66.7%) had moderate PR with combined Ps; those with homograft PA conduit, associated with TI (moderate degree) **(Table 3).**

Late gadolinium enhancement was performed in 72% of cases (n=24) to assess the myocardial viability. 21% of them (n=5) revealed significant late gadolinium enhancement, two of them after Norwood Op and TCPC repair of single ventricle showing transmural enhancement at the lateral wall of function ventricle. Three of them after TAP repair of TOF in the area of insertion of the RV at the IVS associated with hypokinesia **(Table 4).**

Table (1): Diagnosis & type of operation of participants of post d-TGA repair, single ventricle repair, post TOF repair and rest post-surgical participants

	Variables		No (%)
post d-TGA repair	**Diagnosis**	TGA	3 (60 %)
		DORV TGA type	2 (40 %)
	Type of operation	Arterial switch LeCompte- maneuver	4 (80 %)
		Atrial switch	1 (20 %)
single ventricle repair	**Diagnosis**	Single vent. HLHS	5 (55.6 %)
		Single Ven HRHS	2 (22.2 %)
		Single Ven DILV	1 (11.1 %)
		Single Ven DORV	1 (11.1 %)
	Type of operation	Three staged Norwood operation	6 (66.7 %)
		TCPC	3 (33.3 %)
	Aortic arch reconstruction at ISTA	No	3 (33.3 %)
		Reconstruction Plastic patch	6 (66.7 %)
	Stent	No	7 (77.8 %)
		LPA	2 (22.2 %)
post TOF repair	**Diagnosis**	TOF	13 (92.8 %)
		DORV TOF type	1 (7.2 %)
	Type of operation	TAP transannular Patch (Fallot)	12 (85.7 %)
		Conduit in PA position as 1ry intervention	2 (14.3 %)
		Homograft	1
		Stented Xenograft	1
	Reintervention post TOF	No	10 (71.4 %)
		PA branch stent	2 (14.2 %)
		PA valve replacement (Melody)	1 (7.2 %)
		Conduit graft in PA position (homograft)	1 (7.2 %)
rest post-surgical participants	**Diagnosis**	Con Ao valve Stenosis	3 (60 %)
		PA with VSD	1 (20 %)
		ASD	1 (20 %)
	Type of operation	Ross operation	3 (60 %)
		Lt mBT	1 (20 %)
		Repair of ASD	1 (20 %)
	Extra Conduit in PA position (in Ross Operation)	Homograft	2 (40 %)
		Stented Xenograft	1 (20 %)
	Additional Stent	RPA	1 (20 %)

Table (2): Summarizing the different complications detected in the different post-surgery interventions performed in various CHD

CHD	No.	Surgical intervention	No.	Complications	No.
TGA	**5**	Arterial switch LeCompte-maneuver	**4**	Re isthmus stenosis, with PA valve stenosis	1(20%)
				PA artery stenosis	1 (20%)
				LV dysfunction	2(40%)
		Atrial switch	**1**	RVD and RV dysfunction	1(20%)
TCPC	**9**	Norwood Op. and TCPC	**6**	Functional ventricle dysfunction	3(33%)
				Dilation of the neu aorta	5 (55%)
				lesion at prior conduit/shunt sites	2 (22%)
		TCPC	**3**	Functional ventricle dysfunction	1(11%)
				Dilation of aorta	2 (22%)
Post TOF	**14**	TAP transannular Patch	**10**	PA regurgitation	10 (71%)
				Additional PA valve stenosis	4 (29%)
				PA branch stenosis	3(21%)
				RV dilation	9(64%)
				RV dysfunction	4(28%)
		Conduit	**3**	PA regurgitation	2(14%)
				Additional Conduit Stenosis	1(7%)
		Melody PA valve replacement	**1**	No complication	
Diff operation	**5**				
Congenital aortic valve stenosis	**3**	Ross operation	**3**	Ectasia Aorta	3 (100%)
				Combined PA valve regurgitation and stenosis	2(66.6%)
				RV dysfunction	1(33.3%)
				RV dilatation with TI	2(66.6%)
P.atresia with VSD	**1**	Lt mBT	**1**	Biventricular dilation, LV myocardial fibrosis, Aortic ectasia	1(100%)
ASD	**1**	ASD closure	**1**	No complication	

Table (3): Valve lesions after different surgical repair of the participants

Post TGA repair	**PR**		3 (60 %)
	Degree	Trivial	2 (40 %)
		Mild	1 (20 %)
	PS		1 (20 %)
	AR		4 (80 %)
	Degree	Trivial	3 (60 %)
		Mild	1 (20 %)
	AS		0 (0 %)
	TI		3 (60 %)
	Degree	Mild	2 (40 %)
		Moderate	1 (20 %)
	MI		3 (60 %)
	Degree	Trivial	1 (20 %)
		Mild	2 (40 %)

Single ventricle repair	**AR**		5 (55.6 %)
	Degree	Trivial	5 (55.6 %)
	AS		0 (0 %)
	TI	Yes	3 (33.3 %)
		Atresia /closed	2 (22.2 %)
	Degree	Trivial	1 (11.1 %)
		Mild	1 (11.1 %)
		Moderate	1 (11.1 %)
	MI	Yes	2 (22.2 %)
		M atresia	2 (22.2 %)
	Degree	Trivial	1 (11.1 %)
		Severe	1 (11.1 %)
Post TOF repair	**PR**		12 (85.7 %)
	Degree	Mild	1 (7.1 %)
		Moderate (20-40)	4 (28.6 %)
		Severe (>40)	7 (50 %)
	PS		5 (35.8 %)
	AR		5 (35.8 %)
	Degree	Trivial	3 (21.5 %)
		Mild	2 (14.3 %)
	TI		10 (71.4 %)
	Degree	Mild	5 (35.6 %)
		Moderate	2 (14.3 %)
		Severe	3 (21.5 %)
	MI		6 (42.9 %)
	Degree	Trivial	1 (7.1 %)
		Mild (0-20)	5 (35.8 %)
	AS		0 (0 %)
Ross operation	**PR**		2 (66.7 %)
	Degree	Moderate	2 (66.7 %)
	PS		2 (66.7 %)
	AR		3 (100 %)
	Degree	Trivial	1 (33.3 %)
		Mild	2 (66.7 %)
	TI		2 (66.7 %)
	Degree	Moderate	2 (66.7 %)
	MI		3 (100 %)
	Degree	Trivial	2 (66.7 %)
		Mild (0-20)	1 (33.3 %)
	AS		0 (0 %)

Table (4): LGE in 33 post-surgical cases

Variables		**No (%)**
LGE sequence	**Not done**	9 (27.3 %)
	Done	24 (72.7 %)
Site of enhancement	**No enhancement**	16 (66.6 %)
	Ventricular free wall	2 (8.2 %)
	LV wall	2 (8.2 %)
	RV free wall and insertion points	3 (12.5 %)
	LV wall, septum	1 (4.1 %)

LGE: Late gadolinium enhancement, LV: Left ventricle, RV: Right ventricle

Case 1: Cardiac underlying disease: complex transposition of the large arteries (D-TGA) with VSD, underwent corrective surgery of ASO of LeCompte manoeuver. **Figure (1)**

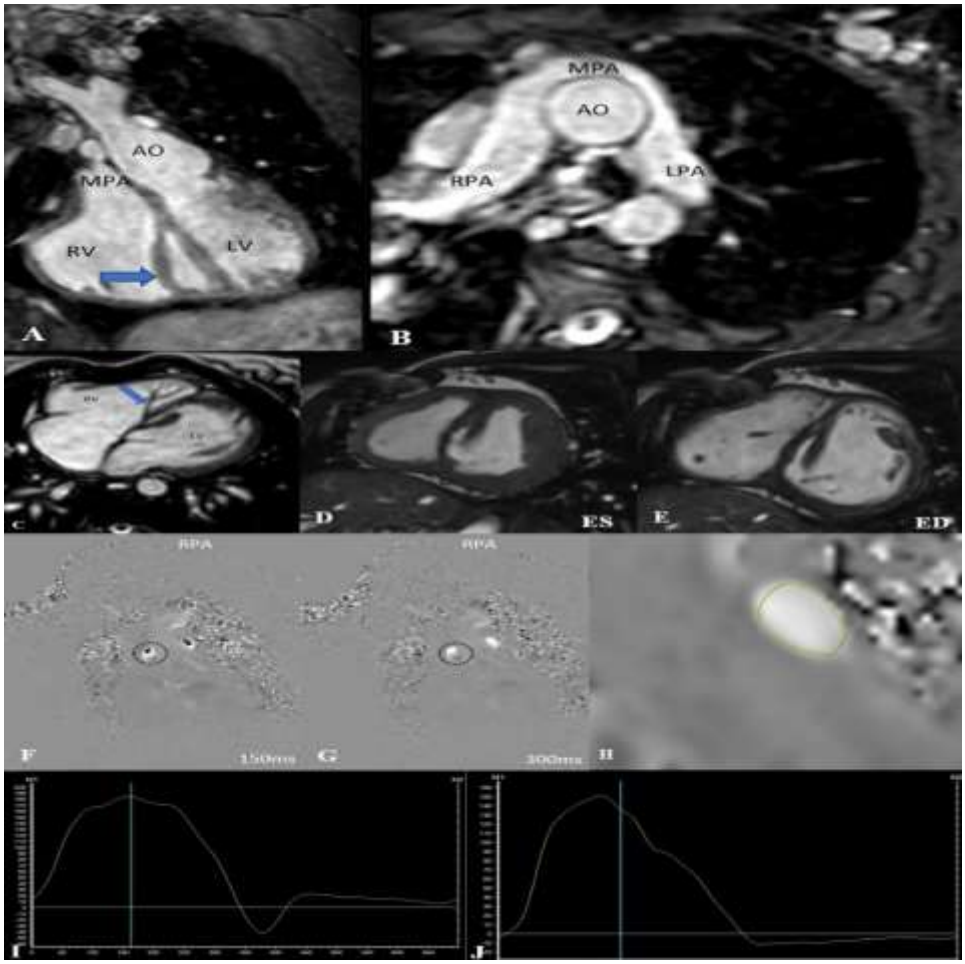

Figure (1): CMR images (A): Oblique coronal reformatting view from 3D SSFP through the ventricular outflow tracts showing the aorta arising from the left ventricle (LV) and the pulmonary trunk form the right ventricle (RV) (with its characteristic moderator band (arrow). (B): Axial reformatting image show the pulmonary artery anterior to the ascending aorta (AAo). (C): Cine SSFP 4CH view shows all four chambers of heart are normal. Mid ventricular SA image in ES (D) and ED (E) show slightly reduced LV function with somewhat reduced inward movement of the IVS. Velocity-encoded phase-contrast which illustrate flow obtained perpendicular to the RPA (tp), (F and G) in which was aliasing with 150cm/s as in (F) and disappear with increasing velocity to 300 cm/s in (E). While (H) VEC image through the LPA show normal intense signal reflecting the antegrade flow with no aliasing. (I and J) Graph flow measurements demonstrating moderately prox. RPA stenosis of about 30%, flow acceleration to 2.6 m/s with forward flow 48 ml and RF 4% (I) while LPA no stenosis with forwards flow (30 ml) and RF 8% (J). RPA/LPA flow ratio: 1.7:1.

Case 2: CMR images of a patient with d-transposition of the great arteries and sub pulmonary fibro muscular outflow tract obstruction. Underwent Atrial switch Operation (Senning Procedure), xenograft implantation at pulmonary artery bifurcation and connection at the apex of the left ventricle**. Figure (2)**

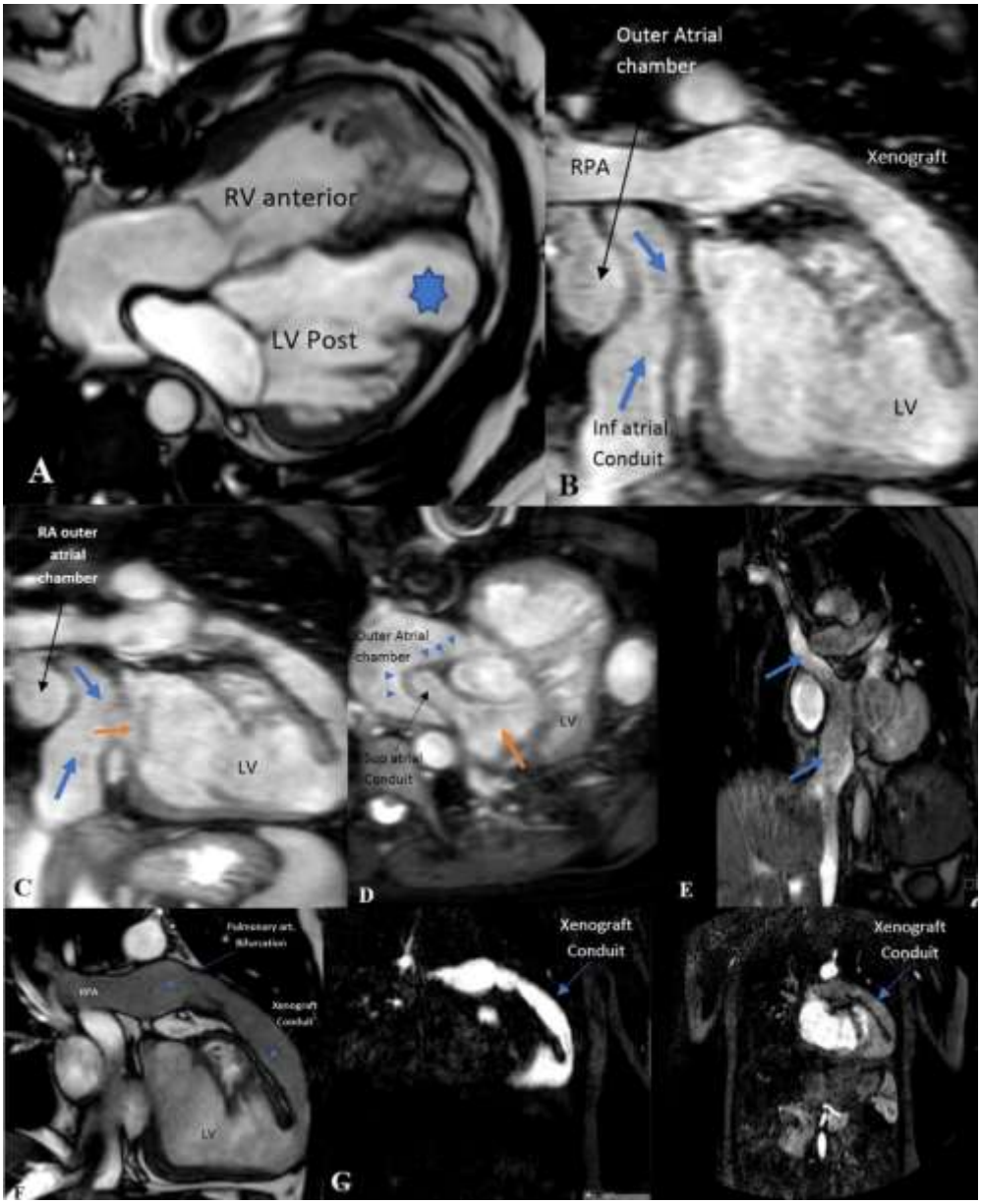

(A): Cine four-chamber SSFP view shows relative dilated RV (NB. Star; Bulge from the connection of Xenograft from the apex of LV to pulmonary bifurcation). All images **(B-D)** taken from frames of 3D balanced SSFP data. **(B, C):** Oblique coronal view shows superior, inferior atrial conduits and common conduit directed to the left atrium and then to the LV. **(D):** Oblique axial view showing superior systemic venous pathway joining to rim of mitral valve (orang arrow) and connecting into left ventricle. Images also clearly show conduits forming inner venous atrial chamber, separate from systemic outer atrial chamber (Line of separation arrow heads). **(E):** Sagittal cine SSFP shows patent superior and inferior atrial conduits (blue arrow). **(F):** Cine sagittal view of the Xenograft conduit from left ventricle to pulmonary artery bifurcation demonstrating patent lumen which further shown by dynamic gadolinium contrast imaging (sagittal image in **(G).**

Case 3: Underlying disease: Hypoplastic left heart. After modified Norwood operation I-III with TCPC, aortic arch reconstruction and stenting at LPA. **Figure (3)**

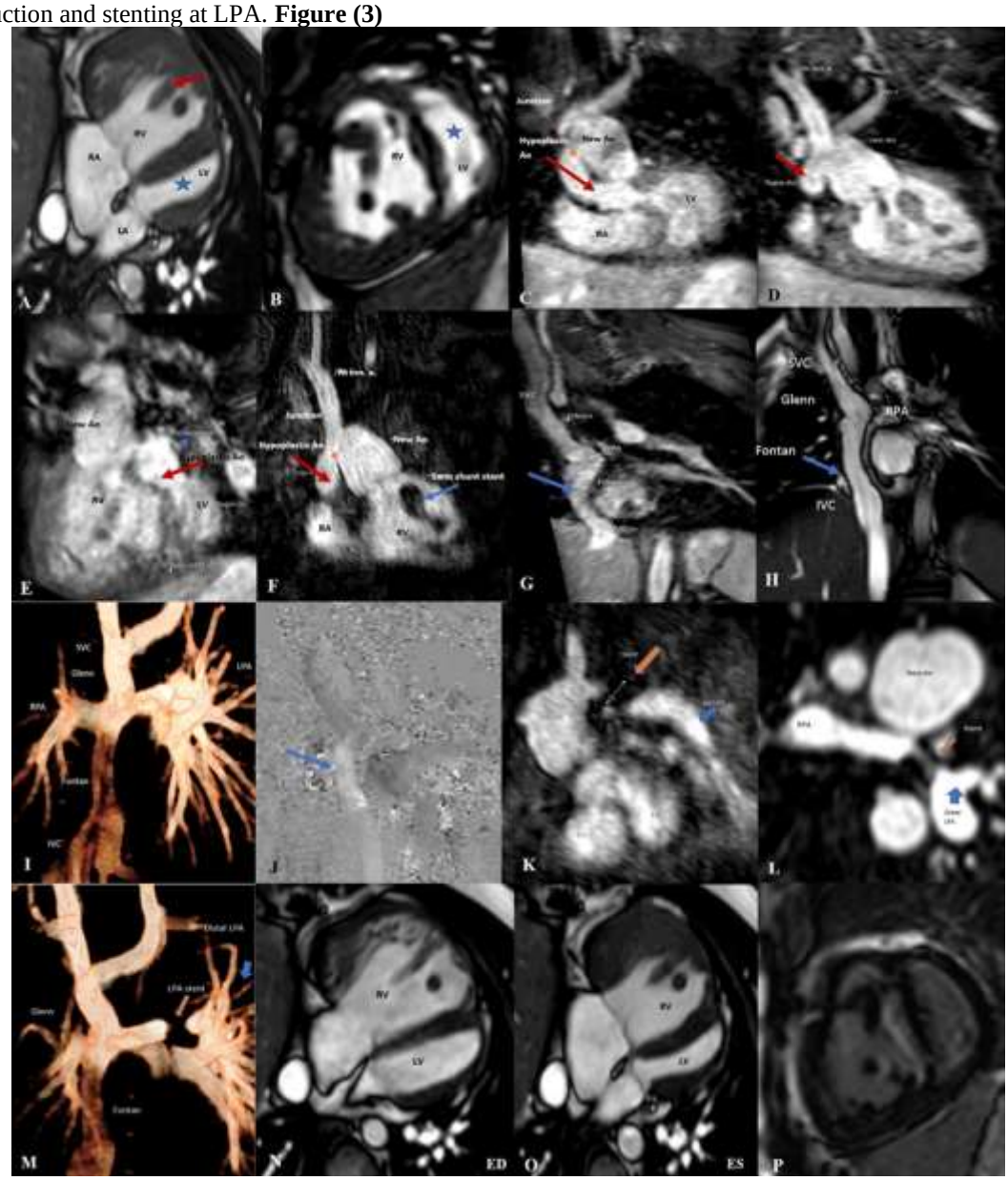

Figure 3: Demonstrating hypoplastic left ventricle (*) on four-chamber view **(A)** with ASD (arrow), hypoplastic left ventricle (*) seen on short axis **(B),** and hypoplastic aorta (red arrow) on coronal (**C, D**), sagittal oblique (**E)** 3D SSFP image (**C-E**). The 3D SSFP different reformatting images in (**C-E**) as well as Gadolinium-enhanced angiography image (**F**) showed hypoplastic left ventricle, narrow caliber and hypoplastic native aorta (red arrow) with an anastomosis to the new-aorta (orange arrow). (**G**): Sagittal Oblique 3D SSFP shows TCPC which involves the anastomosis of both the SVC and the IVC to the RPA with extracardiac Fontan conduit (arrow). (**H**): Coronal SSFP cine, (**I**) 3D volume rendering images shows patent lumen of extracardiac TCPC conduit. (**J**): VEC phase contrast image (**ip**) along the TCPC showed no evidence of thrombi in the conduit or within the Fontan circulation flow. LPA with multiple stents, intraluminally assessable neither angiographically (**K**) nor natively (3D axial) (**L**) as well as in 3D volume rendering image (M) due to susceptibility artefacts. However, the contrast agent crossed over into the peripheral left pulmonary arteries. Cine 4CH SSFP (**N in ED**) and (**O in ES**) showed slightly enlarged and severely hypertrophied right systemic ventricle with mildly impaired function (RV-EF 43%). (**P**): SA image in LGE sequence showed no evidence of myocardial fibrosis, necrosis, or scar.

Case 4: Fallot patient with pulmonary atresia and VSD after implantation of a valve-bearing conduit (biological conduit). MRI done for quantification of RV and LV size and Function, PI as well as diameter of pulmonary branches, and if myocardial scars present**. Figure (4)**

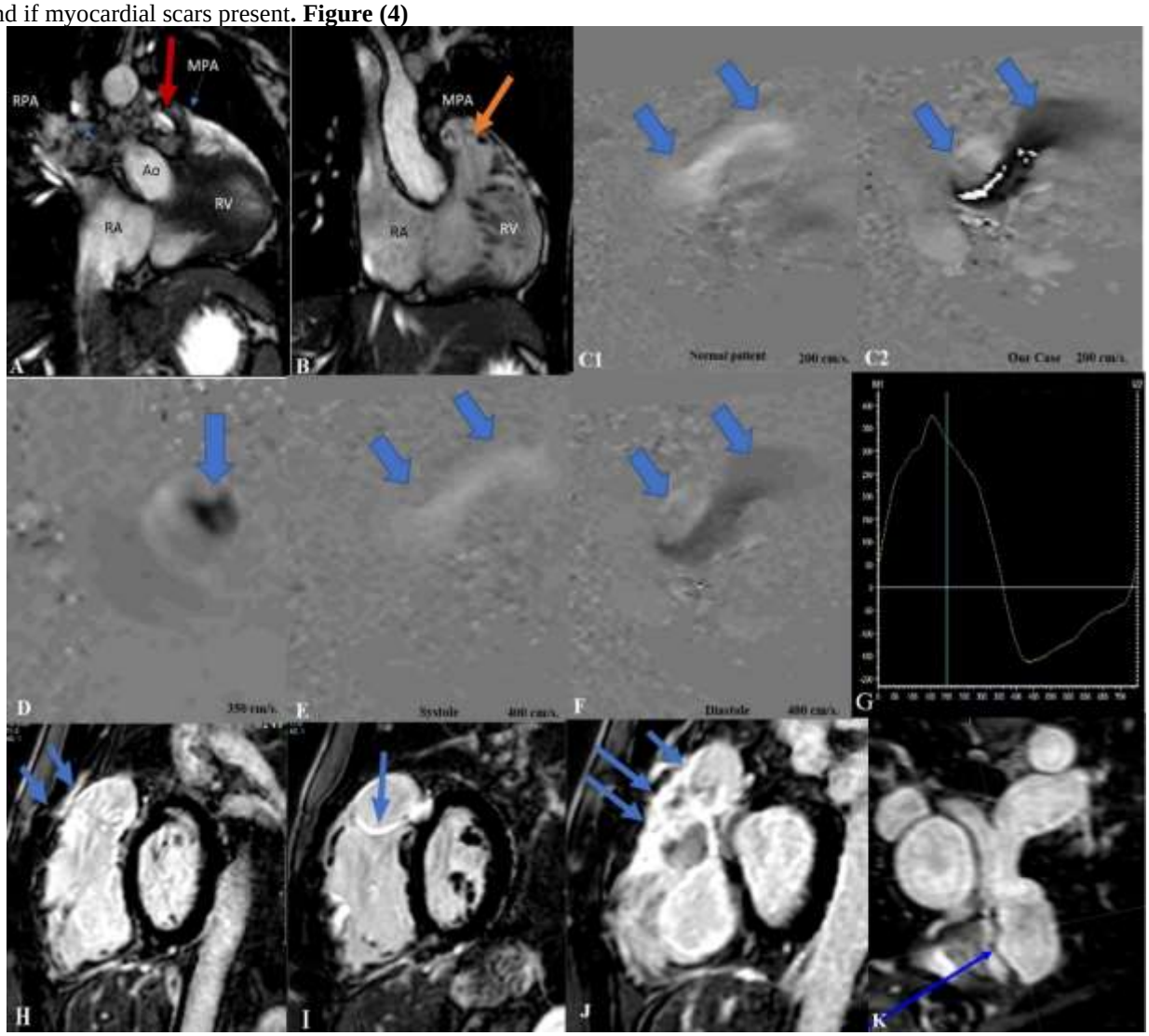

Figure (4): Dynamic cine MR images of the heart, obtained with SSFP, provide longitudinal axis view at the level of the RVOT. Residual valvular stenosis is indicated by a jet of low signal intensity during systole **(A)** (red arrow) and by valvular regurgitation during diastole **(B)** (orange arrow). Phenomenon of aliasing seen in the In-plane velocity mapping of the MPA panel **(C)** shows the phase image during systole with Venc set at 200 cm/s. Systolic forward is normally displayed as normal white as in **(C1),** but in our case **(C2)** a jet core has coherent laminar flow (arrowed) corresponds to the region of highest velocity, this means that the peak velocities have exceeded the Venc. (**D**) shows a second acquisition with Venc set at 350 cm/s, there is still slight aliasing in through plane mapping. **(E)** shows a third acquisition during systole with Venc set at 400 cm/s, eliminating the aliasing effect. **(F)** During diastole the reduced signal reflects retrograde flow due to regurgitation; **(G):** graph showing pulmonary valve flow during a cardiac cycle; showing anterograde flow of 90 mL and retrograde flow 36 mL representing a regurgitation fraction of 40%. Vmax 3.0 m/s. SA late gadolinium enhancement (LGE) image of the arrows indicate enhancement at insertion site of conduit, (**H-J).** (**K**): Axial 3D SSFP images showing Conduit insertion points with thickened wall.

Discussion

All 33 cases (71.7%) were referred for post-surgery evaluation. This going with van der Hulst et al., 2012 [9] and Pennell et al. [10] that stated that In the clinical follow-up of postoperative CHD cases, cardiac MRI (CMRI) is a crucial non-invasive imaging technology. CMRI is not hindered by geometrical assumptions or the acoustic window, which can restrict echocardiographic imaging in cases with postoperative CHD due to aberrant cardiac anatomy or scarring.

The subgroups of our postoperative cases included 5 cases after correction of d-transposition of the great vessels, 9 cases undergoing single ventricle repair , 14 cases post TOF repair, and 5 cases with other different operations, this agreed with Fratz et al. [11] and Roest et al. [12] who reported that the most frequent categories of postoperative CHD cases designated for CMRI assessment are those with coarctation of the aorta, TGA, and single ventricle after Fontan intervention. The different categories necessitate distinct CMRI protocols based on postoperative anatomy and the particular medical problems that may arise during follow-up. [9]

CMRI is rarely required for before intervention assessment of infants with D-loop TGA as Echo usually offers all necessary diagnostic data. In post-surgery TGA, CMRI acquires an increasing role due to its capacity to evaluate most clinically related problems. [13]

We reached to the same conclusion in our research; the cases with D-TGA referred for MRI were post-surgery and our goals in CMRI evaluation were the same with the research of Nielsen and his colleagues, 2007 evaluations of the left and right ventricular outflow tract (RVOT) and TR were performed, as were evaluations of RV size and function. for narrowing and detection of aortic or PA collaterals. Myocardial Fibrosis can be identified by the presence of post-gadolinium MDE. [14]

MRI is frequently used to evaluate the anatomy and function of FSV cases who have undergone surgery. Recent research by Johnson et al. [15] indicates that before intervention MRI can offer details not discovered by Echo alone that has the ability to modify the treatment plan.

Cardiac MRI played an important role in detection post-surgery complication as following, as regard the first in our research, surgically repaired congenital cardiac disease was post-d-TGA repair. In one case, the Senning atrial switch was utilized, and in four cases, the ASO (Le Compete maneuver) was conducted. The Senning intervention was performed on a case with a dilated RV (EDV/BSA = 110 ml/m2), moderate TI (30%RF), and a reduced RVEF (EF = 40%), indicating right ventricular failure. Saraya et al. [16] described comparable post-surgery findings and ascribed them to the continuous exposure of the RV to systemic pressure, which ultimately led to compensatory hypertrophy and ventricular failure.

In our research, the four cases after ASOs revealed complications as PA branch stenosis (20% of cases n= one case), LV dysfunction (EF of average 48% in 40% of cases n = 2) and reisthmus stenosis with PA valve stenosis (in 20% n = 1), while Saraya et al. [16] reported no significant complications in their research after ASO. However several studies including Cohen et al. [17] reported problems after the ASO include narrowing of the coronary arteries, AR and dilatation of the proximal AAO and the LV as well as PA stenosis, which occurs 25% of cases. Ou et al. [18] found another interesting finding that the most frequent complication of the ASO is PA branch stretching that rarely leads to significant stenosis.

Shepard et al. [19] found that majority of cases after arterial switch had normal LVEDVs and RVEDVs. However, 26% had LV dilation (severe in only 1.1%) and 20% had RV dilatation (none was severe). In Our research one case (20%) reported with LV dilation (EDV/BSA 126 ml/m²) while (100%) after ASO showed normal RV function and size.

According to the valve lesions in post TGA cases our research revealed, three cases (60%) had PR (RF less than 20%) after ASO, 20% (n=1) had combined PS with V max 3m/s and PI with RF 17%. AR found in all cases post ASO but of non-significant degree with RF less than 20% this consistent with aortic dilatation. No case had AS. Regarding the atrio ventricular valves in post TGA repair 60% of the cases (n=3 cases) had TI; two less than 20% RF and the one after Atrial switch developed moderate TI (RF30%).

Among 206 cases with proximal aortic flow readings, 118 (57.3%) had no or minimal neo AR (RF 5%), 35.0% had mild neo AR (RF 25-40%), and 7.7% had severe neo AR (RF >20%), as determined by the criteria established by Shepard et al. [19]. Similarly, PR was found to be absent or minimal in 105 (59%) of the cases, mild in 57 (32%) of the cases, and moderate or severe in 16 (9%) of the cases.

In interventions for single ventricle repair (9 cases), the following complications were detected in ours; functional ventricular dysfunction in 44% (n=4) and 22% (n=2) showed lesions in previous site of operation as LSA occlusion from previous mBT and re isthmus stenosis. Near total cases of single ventricle repair (77%) developed dilation of new/ native aorta. Patent TCPC with no stenosis or thrombosis found in 100% of cases. Navarro-Aguilar et al. [20] reported that the potential cardiac complications post FSV repair are ventricular dysfunction, atrioventricular valve regurgitation, and complications of the conduit. This disagreed with Saraya et al., [16] who reported no complications were detected in any of the performed repair interventions of Single ventricle. This consistent with our research as regard the total cavo-PA shunt itself, which showed patent lumen with no stenosis or thrombosis in all cases 100%.

In our research, the post-surgery CMRI evaluation criteria for total TOF repair included RV volume, RVEF, PR fraction (RF), and LV volume and function. In addition, the development of patch dilatation and PA branch stenosis was evaluated. This agreed with the research by Mercer-Rosa et al., [21] and Saraya et al. [16].

Our findings revealed that PR was the most frequent complication (85.7% from all post TOF, n=12), 7 of them (50%) of severe grade (RF> 40 %), 28.6% of them (n=4 cases) showed moderate grade. This is a significant percentage compared to the 30% of cases where PR was present in Saraya et al., 2020 [16] research but in consistent with the research of Mercer-Rosa et al., 2012 [21] research (90% of cases) was detected showing PR post-operatively.

Regarding RV dilatation and failure after TOF repair, Vaujois et al. [22] 80% of cases were discovered to have at least moderate to severe PR, leading to RV overburden, progressive dilation, and failure. In addition, progressive RV dilatation frequently results in tricuspid valve annulus elongation and subsequently TR, which exacerbates RV dilatation. In addition, concomitant conditions that increase PA systolic pressure, such as branch PA stenosis, LV failure, and acquired PA disorders, aggravate PR and its effect on the RV.

In our research following TOF repair, we detected 28.5% of cases (n=4) with RV dysfunction associated with RV dilatation after TAP operation with one of them (EF 22% and EDV/BSA 182 ml/m2) showed additionally myocardial fibrosis as a sign of right ventricular stress. Right ventricular dilation found in 64% of them (n=9) with six cases had marked dilation (EDV/BSA more than 150 ml/m2); five of them with significant TR (35.7% n=5). This agreed with Saraya et al. [16] and Oosterhof et al. [23] demonstrating those with delayed mural enhancement subsequent to TOF repair had a low RV EF (43% ± 6.3) and large EDV (175 mL/m^2 ± 42).

In our research combined PS and PR found in 40% after TAP (n=4) while PA branch stenosis found in 21% of all 14 cases after TOF repair (n= 3). Saraya et al. [16] showed PA branch stenosis (39%) of which 7 affected the left PA and only 2 affected the right PA.

Ten percent to fifteen percent of individuals undergoing TOF surgery experience RVOT or PA stenosis, as shown by research from Vaujois et al. [22]. You can find stenosis anywhere from the proximal RVOT to the distant PA branches.

As regard the three cases who had conduit in PA position, complications are detected only in the two cases with the homograft type in the form of moderate PR of average 30-35% RF associated-with additional stenosis occurred in one of them but none of them had RV dysfunction or significant RV dilatation. This corroborated the findings of Vaujois et al. [22], who found that infants often require multiple surgical re-operations as a result of the gradual narrowing of the conduit as a result of distal anastomotic stenosis, conduit kinking, extensive intimal proliferation and calcification, extrinsic sternal compression as well, and/or valve regurge.

Geva [24] discovered that PA valve replacement (PVR) should be planned to enhance cardiac hemodynamic. Determining when to perform the PVR is crucial, particularly in young cases due to the limited durability of bio-prostheses and the possibility of repeated PVR.

In our research one case after total correction of TOF and homograft implantation at TP position underwent Melody PA valve replacement due to evidence of failure of the homograft conduit depending upon MRI criteria according to Geva [24] RV dilatation (RV EDV> 150 ml/m2) (RV-EDV/BSA 182 ml/m²), right ventricular ejection fraction (<47%) (EF 22%), large RVOT aneurysm (38mm), PA stenosis with flow acceleration to 4 m/s, moderate TR (30%), however PR showed mild degree with RF 19% according to Geva [24] PR ≥ 25%. Depending upon that PR will be worsened by concomitant proximal PA stenosis as well as right ventricular overload and ventricular dysfunction.

In our research MRI played important role in post Ross operation assessment with detection of complications in the form of conduit combined stenosis (Vmax 4m/s) and moderate regurgitation in (66.7%) representing the two cases with PA homograft type associated with RV dilatation (EDV/BSA 130 ml/m^2 and 140 ml/m^2) combined with TI of 26% RF. However right ventricular dysfunction (EF 44%) was noted in one of them (33%).However aortic bulb ectasia of average 45 mm shown in all post Ross cases (100%) with non-significant AR (RF less than 20%).

This going with the research of Grotenhuis et al. [25], as in their prospective research revealed the imaging mild degrees of homograft stenosis in cases after the Ross intervention.

Following a palliative LtmBT shunt which performed in a case with PA atresia in our research the following assessment showed biventricular significant dilation (EDV/BSA162 ml/m² and 168 ml/m² in LV and RV respectively) with slight LV dysfunction (EF 50%) associated with scattered myocardial fibrosis. However, no complication was detected as regard the mBT itself as well as PAs and aortopulmonary collaterals vessels. This was against the research of Saraya et al. [16], which included 11 MBT shunts performed in DORV and PA stenosis cases of which 3 were totally obstructed.

LGE was performed in 24 cases of our post-surgery cases to assess the myocardial viability.

In the research of Rathod et al.[26], LGE has been observed in 28% of Fontan operation (FO). The unrestricted wall of the primary ventricle is the most frequent site of LGE after a FO (64%). This consistent with our research after FO; 28.5 % of cases (n=2 from 7 cases who had this sequence) has significant LGE; along the lateral (free) wall of functional ventricle with transmural pattern of enhancement, while two cases showed non-significant enhancement with speckled pattern and the rest showed no enhancement.

Ylitalo et al. [27] observed in TOF some LGE is typically seen at the site of operation in the RVOT, especially after transannular patch restoration, but sometimes it extends well beyond the surgical site and involves any of the RV wall, most frequently the anterior wall. In our research three cases after TAP significant transmural enhancement in the RV free wall as well as in the area of insertion of the RV at the IVS associated with hypokinesia.

Limitations:

Number of research cases might not have been large enough to provide statistical significance; the research lacked a true gold standard for comparison. Long scan time, suboptimal imaging in case of arrhythmia, and susceptibility to respiratory artifacts also represented some limitations.

Conclusions:

CMRI provides a powerful non-invasive imaging tool, giving anatomic and haemodynamic information that echo and catheterization alone do not provide. It surpasses both catheterization and echo in its ability to create high resolution, three-dimensional reconstructions of complex CHD. CMRI eliminates with the need for contrast media which are bound by dose-restrictions in the assessment of paediatrics due to their nephrotoxicity and other potential adverse effects, which encouraged CMRI application not only in pre-surgical planning, but also during post-surgery follow up of CHDs. While evaluating the present function of cardiac MRI in the assessment of CHD, it is important to consider the limitations of the technology, which include its high price and low availability, as well as the need for appropriate sedation, which may involve general anesthetic.

Financial support and sponsorship: Nil

Conflict of Interest: Nil

List of abbreviation:

AAO: Ascending aorta. **Ao**: Aorta. **AR**: Aortic regurgitation. **AS**: Aortic stenosis. **ASD**: Atrial septal defects. **ASO**: Arterial switch operation. **BMI**: Body mass index. **BT**: Blalock–taussig. **CA**: Coronary arteries. **ceMRA**: Contrast enhanced MR-angiography. **CHD**: Congenital heart disease. **DILV**: Double inlet left ventricle. **DORV**: Double outlet right ventricle. **D-TGA**: Dextroposed transposition of the great arteries. **Echo:** echocardiography. **ED**: End diastole. **EDV**: End-diastolic volume. **EF**: Ejection fraction. **ES**: End systole. **ESV**: End-systolic volume. **FSV**: Function single ventricle. **Gd-DTPA**: Gadolinium-diethylenetriamine pentaacetic acid. **HLHs**: Hypoplastic left heart syndrome. **HRHS**: Hypoplastic right heart syndrome. **ISTA**: Isthmus stenosis of the aorta. **IVC**: Inferior vena cava. **IVS**: Interventricular septum. **LA**: Left atrium. **LGE**: Late gadolinium enhancement. **LPA**: Left pulmonary artery. **LSCA**: Left subclavian art. **LV**: Left ventricle. **mBT**: Modified blalock-taussig shunt. **MDCT**: Multi detector CT. **MI**: Mitral incompetence. **MPA**: Main PA artery. **MR**: Magnetic resonance. **MS**: Mitral stenosis. **PC**: Phase-contrast. **PI**: pulmonary incompetence. **PR:** pulmonary regurgitation. **TOF:** Tetralogy of Fallot. **PS:** pulmonary stenosis. **RVOT:** Right ventricular outflow tract. **TR:** Tricuspid regurgitation.

References:

1. Marelli AJ, Mackie AS, Ionescu-Ittu R, Rahme E, Pilote L. Congenital heart disease in the general population: changing prevalence and age distribution. Circulation. 2007;115:163-72.
2. Hopewell NN, Hughes ML, Taylor AM. The role of cardiovascular magnetic resonance in pediatric congenital heart disease. J Cardiovasc Magn Reson. 2011;13:51.
3. Prakash A, Powell AJ, Geva T. Multimodality noninvasive imaging for assessment of congenital heart disease. Circ Cardiovasc Imaging. 2010;3:112-25.
4. Atallah J, Dinu IA, Joffe AR, Robertson CM, Sauve RS, Dyck JD, et al. Two-year survival and mental and psychomotor outcomes after the Norwood intervention: an analysis of the modified Blalock-Taussig shunt and right ventricle-to-PA artery shunt surgical eras. Circulation. 2008;118:1410-8.
5. Ho VB, Kinney JB, Sahn DJ. Contributions of newer MR imaging strategies for congenital heart disease. Radiographics. 1996;16:43-60; discussion 1.
6. Dorfman AL, Levine JC, Colan SD, Geva T. Accuracy of Echo in low birth weight infants with congenital heart disease. Pediatrics. 2005;115:102-7.
7. Lai WW, Geva T, Shirali GS, Frommelt PC, Humes RA, Brook MM, et al. Guidelines and standards for performance of a pediatric echocardiogram: a report from the Task Force of the Pediatric Council of the American Society of Echo. J Am Soc Echocardiogr. 2006;19:1413-30.
8. Marcotte F, Poirier N, Pressacco J, Paquet E, Mercier LA, Dore A, et al. Evaluation of adult congenital heart disease by cardiac magnetic resonance imaging. Congenit Heart Dis. 2009;4:216-30.
9. van der Hulst AE, Roest AA, Westenberg JJ, Kroft LJ, de Roos A. Cardiac MRI in postoperative congenital heart disease cases. J Magn Reson. 2012;36:511-28.
10. Pennell DJ, Sechtem UP, Higgins CB, Manning WJ, Pohost GM, Rademakers FE, et al. Clinical indications for cardiovascular magnetic resonance (CMRI): Consensus Panel report. Eur Heart J. 2004;25:1940-65.
11. Fratz S, Hess J, Schuhbaeck A, Buchner C, Hendrich E, Martinoff S, et al. Routine clinical cardiovascular magnetic resonance in paediatric and adult congenital heart disease: cases, protocols, questions asked and contributions made. J Cardiovasc Magn Reson. 2008;10:1-6.
12. Roest AA, Helbing WA, van der Wall EE, de Roos A. Postoperative evaluation of congenital heart disease by magnetic resonance imaging. J Magn Reson. 1999;10:656-66.
13. Videlefsky N, Parks WJ, Oshinski J, Hopkins KL, Sullivan KM, Pettigrew RI, et al. Magnetic resonance phase-shift velocity mapping in pediatric cases with PA venous obstruction. J Am Coll Cardiol. 2001;38:262-7.
14. Nielsen JC, Powell AJ. Cardiovascular MRI applications in congenital heart disease. Indian J Radiol Imaging. 2007;17.
15. Johnson JT, Molina KM, McFadden M, Minich LL, Menon SC. Yield of cardiac magnetic resonance imaging as an adjunct to Echo in young infants with congenital heart disease. Pediatr Cardiol. 2014;35:1067-71.
16. Saraya S, Woodard P, Bhalla S, Gutierrez F, Saraya M, Soliman HH. Cardiac MRI in evaluation of post-surgerycongenital heart disease and complications. Egypt J Radiol Nucl Med. 2020;51:1-12.
17. Cohen MS, Eidem BW, Cetta F, Fogel MA, Frommelt PC, Ganame J, et al. Multimodality imaging guidelines of cases with transposition of the great arteries: a report from the American Society of Echo developed in collaboration with the Society for Cardiovascular Magnetic Resonance and the Society of Cardiovascular Computed Tomography. J Am Soc Echocardiogr. 2016;29:571-621.
18. Ou P, Iserin L, Raisky O, Vouhe P, Brunelle F, Sidi D, et al. Post-surgerycardiac lesions after cardiac surgery in childhood. Pediatr Radiol. 2010;40:885-94.

19. Shepard CW, Germanakis I, White MT, Powell AJ, Co-Vu J, Geva T. Cardiovascular magnetic resonance findings late after the arterial switch operation. Circ Cardiovasc Imaging. 2016;9:e004618.
20. Navarro-Aguilar V, Flors L, Calvillo P, Merlos P, Buendía F, Igual B, et al. Fontan intervention: imaging of normal post-surgical anatomy and the spectrum of cardiac and extracardiac complications. Clin Radiol. 2015;70:295-303.
21. Mercer-Rosa L, Yang W, Kutty S, Rychik J, Fogel M, Goldmuntz E. Quantifying PA regurgitation and right ventricular function in surgically repaired TOF: a comparative analysis of Echo and magnetic resonance imaging. Circ Cardiovasc Imaging. 2012;5:637-43.
22. Vaujois L, Gorincour G, Alison M, Déry J, Poirier N, Lapierre C. Imaging of postoperative TOF repair. Diagn Interv Imaging. 2016;97:549-60.
23. Oosterhof T, Mulder BJ, Vliegen HW, de Roos A. Corrected TOF: delayed enhancement in RVOT. Radiology. 2005;237:868-71.
24. Geva T. Repaired TOF: the roles of cardiovascular magnetic resonance in evaluating pathophysiology and for PA valve replacement decision support. J Cardiovasc Magn Reson. 2011;13:1-24.
25. Grotenhuis HB, de Roos A, Ottenkamp J, Schoof PH, Vliegen HW, Kroft LJ. MR imaging of right ventricular function after the Ross intervention for aortic valve replacement: initial experience. Radiology. 2008;246:394-400.
26. Rathod RH, Prakash A, Kim YY, Germanakis IE, Powell AJ, Gauvreau K, et al. Cardiac magnetic resonance parameters predict transplantation-free survival in cases with fontan circulation. Circ Cardiovasc Imaging. 2014;7:502-9.
27. Ylitalo P, Pitkänen OM, Lauerma K, Holmström M, Rahkonen O, Heikinheimo M, et al. Late gadolinium enhancement (LGE) progresses with right ventricle volume in children after repair of TOF. IJC Heart Vessel. 2014;3:15-20.